University of Plymouth

PEARL **https://pearl.plymouth.ac.uk**

01 University of Plymouth Research Outputs University of Plymouth Research Outputs

2017-06-01

Systematic analysis of rocky shore platform morphology at large spatial scale using LiDAR-derived digital elevation models

Matsumoto, H

http://hdl.handle.net/10026.1/9102

10.1016/j.geomorph.2017.03.011
Geomorphology
Elsevier BV

All content in PEARL is protected by copyright law. Author manuscripts are made available in accordance with publisher policies. Please cite only the published version using the details provided on the item record or document. In the absence of an open licence (e.g. Creative Commons), permissions for further reuse of content should be sought from the publisher or author.

Systematic analysis of rocky shore platform morphology at large spatial scale using LiDAR-derived digital elevation models

Authors: Hironori Matsumoto[1]*, Mark E. Dickson[1], Gerd Masselink[2]

[1]School of Environment, The University of Auckland, Private Bag 92019, Auckland 1142, New Zealand
[2]School of Marine Science and Engineering, Plymouth University, Drake Circus, Plymouth, Devon PL4 8AA, United Kingdom

Corresponding author at: School of Environment, The University of Auckland, Private Bag 92019, Auckland 1142, New Zealand.

Email Address: hmat258@aucklanduni.ac.nz (H. Matsumoto)

Abstract
Much of the existing research on rocky shore platforms describes results from carefully selected field sites, or comparisons between a relatively small number of selected sites. Here we describe a method to systematically analyse rocky shore morphology over a large area using LiDAR-derived digital elevation models. The method was applied to 700 km of coastline in southwest England; a region where there is considerable variation in wave climate and lithological settings, and a large alongshore variation in tidal range. Across-shore profiles were automatically extracted at 50 m intervals around the coast where information was available from the Coastal Channel Observatory coastal classification. Routines were developed to automatically remove non-platform profiles. The remaining 612 shore platform profiles were then subject to automated morphometric analyses, and correlation analysis in respect to three possible environmental controls: wave height, mean spring tidal range and rock strength. As expected, considerable scatter exists in the correlation analysis because only very coarse estimates of rock strength and wave height were applied, whereas variability in factors such as these can locally be the most important control on shoreline morphology. In view of this, it is somewhat surprising that overall consistency was found between previous published findings and the results from the systematic, automated analysis of LiDAR data: platform gradient increases as rock strength and tidal range increase, but decreases as wave height increases; platform width increases as wave height and tidal range increase, but decreases as rock strength increases. Previous studies have predicted shore platform gradient using tidal range alone. A multi-regression analysis of LiDAR data confirms that tidal range is the strongest predictor, but a new multi-factor empirical model considering tidal range, wave height, and rock strength yields better predictions of shore platform gradient (root mean square error of predictions reduced by 5%). The key finding of this study is that large-scale semi-automated morphometric analyses have the potential to reveal dominant process controls in the face of small-scale local variability.

Keywords
LiDAR, DEM, shore platform, rock coast

1. Introduction

A range of landforms occur along rocky shorelines, but particular research attention has been afforded to the distinctive low-gradient intertidal shore platforms that often occur in front of eroding cliffs (e.g. Trenhaile, 1987; Sunamura, 1992). Early studies of shore platform geomorphology were highly descriptive and focussed on a small number of platforms, distinguished in their morphology in some respect (e.g., Dana, 1849; Bartrum, 1926, 1938; Wentworth, 1938; Edwards, 1951). This is because slow rates of morphological change and lack of preserved evidence restricted the application of process-based morphodynamic studies (Trenhaile, 1980; Stephenson, 2000). Likewise, logistics dictated that most researchers could work only at a single field site, or perhaps comparing a small number of field sites.

In spite of such difficulties, there have been several key morphological findings reported in the late 20th Century, including: (1) a conceptual demarcation of two shore platform geometries as well as plunging sea cliffs in relation to the relative force of waves and rock resistance (Tsujimoto, 1987; Sunamura, 1992); and (2) widespread positive correlation between mean shore platform gradient and mean spring tidal range (e.g. Trenhaile, 1987, 1999). However, some key areas of morphodynamic understanding remain unclear. For instance, despite recent work describing how process dominance may change through time (Dickson, 2006; Trenhaile, 2008a, 2008b), it is apparent that the classical long-standing debate over the relative dominance of wave and weathering processes has not been clearly resolved (Stephenson, 2000). Overall, despite a great deal of research, slow developmental trajectories, a very wide range of forcing conditions and local site-specific factors mean that shore platform morphology remains an ambiguous indicator of process (Mii, 1962).

Recent research on shore platforms has seen emphasis move from qualitative to quantitative, facilitated by high-frequency, sensitive and portable measuring devices, including pressure transducers (e.g. Stephenson, 2000; Farrell et al., 2009; Ogawa et al., 2011, 2012, 2016), seismometers (e.g. Adams et al., 2002; Young et al., 2011, 2016; Dickson and Pentney, 2012; Normal et al., 2013), micro-erosion meters (e.g. Stephenson and Kirk,1998, 2000; Kanyaya and Trenhaile, 2005; Swantesson et al., 2006;

Porter et al., 2010a, 2010b, 2010c) and laser scanners (e.g. Swantesson et al., 2006; Lim et al., 2011; Rosser et al., 2013). These studies have begun to provide details on the rates of morphological change and the process regime responsible for these changes. However, it is notable that these studies have continued to be rather local in scale, due to measuring-range constraints. Few studies to date have examined the potential of broad-scale quantitative methods for understanding rocky shore evolution.

LiDAR (light detection and ranging) is now a very widely used geomorphological research tool. On rocky shores, Kennedy et al. (2014) and Duperret et al. (2015) combined LiDAR-derived elevation models with bathymetric data to produce seamless onshore-offshore rocky shore profiles. They demonstrated its usefulness in studying historical erosional events when sea levels are different from today. Along 4.2 km of the North Yorkshire (UK) coast Swirad et al. (2016) used LiDAR data and ortho-photographs to reveal weak correlations between shore platform morphology and various environmental controls, suggesting that further consideration of coastal inheritance and detailed rock resistance representations is required in coastal models. Palamara et al. (2007) used LiDAR-derived terrain models to map 2 km of shore platform in southeastern New Zealand. The technique was capable, with caveats, of automatically discerning the cliff-platform junction, seaward platform edge and an upper erosional surface. Palamara et al. (2007, p946-947) noted that “If ALS data prove useful for mapping shore platform morphology at this [local 2 km] scale, there is an opportunity to consider evolution of rocky coast landforms at the regional scale using a single dataset”.

This study aims to systematically analyse rocky shore platform morphology at large region-wide scales using LiDAR derived digital elevation models (DEMs). Our particular interest is placed on shore platform gradient, width and roughness at an analysis scale afforded by LiDAR-derived DEMs with 1 m resolution. We describe a method to semi-automatically extract shore-normal shore platform profiles and present results from an analysis of approximately ~700 km of southwest England coastline. This coastline is notable particularly in respect to the broad and relatively regular transition in tidal range that occurs from north (more than 10 m spring tidal range at North Devon) to south (around 4 m spring tidal range at South Devon). Many other factors vary across the 700 km expanse of coast, including

rock strength and exposure to wave energy, but the large and regular transition in tidal range supports the establishment of a simple testable proposition: is platform gradient positively correlated with tidal range? The literature suggests that this should be the case (see Trenhaile, 1999), but previous studies have focussed on a relatively small number of shore platform sites that had been specifically selected for analysis due to cross-site variability of factors such as rock structure. Our focus therefore, is to question whether an automated systematic analysis of platform morphology over a broad regional scale will yield similar process relationships to those inferred from prior local site studies.

2. Study area

The southwest region of England is subject to a diverse coastal setting (Fig. 1) with a very large variation experienced both in the wave climate and tidal regime (Scott et al., 2011). The Atlantic Ocean produces a mixture of ocean swell to locally-generated wind waves to most coasts, but the significance of different wave types varies owing to local orientation of the coasts and geographical setting (e.g. Bristol Channel and English Channel) (Fig. 1b). The lithological setting also varies, with resistant igneous rock in part of the north and southwest, in comparison to moderately-hard sedimentary rocks in other places (Fig. 1d) (Clayton and Shamoon, 1998). Tidal regime also varies significantly, but, in contrast to the variability in waves and lithology, the tidal regime varies systematically along the coast with mega-tidal spring tide ranges of 9–10 m around the Bristol Channel and macro-tidal spring tide ranges of around 4 m around the English Channel (Fig. 1c). As a result of such a diverse setting, coastal geomorphology also varies considerably, but most of coasts in southwest England are characterized by large expanses of rocky coastline alternated by embayed beaches, small estuaries and rocky headlands (Scott et al., 2011).

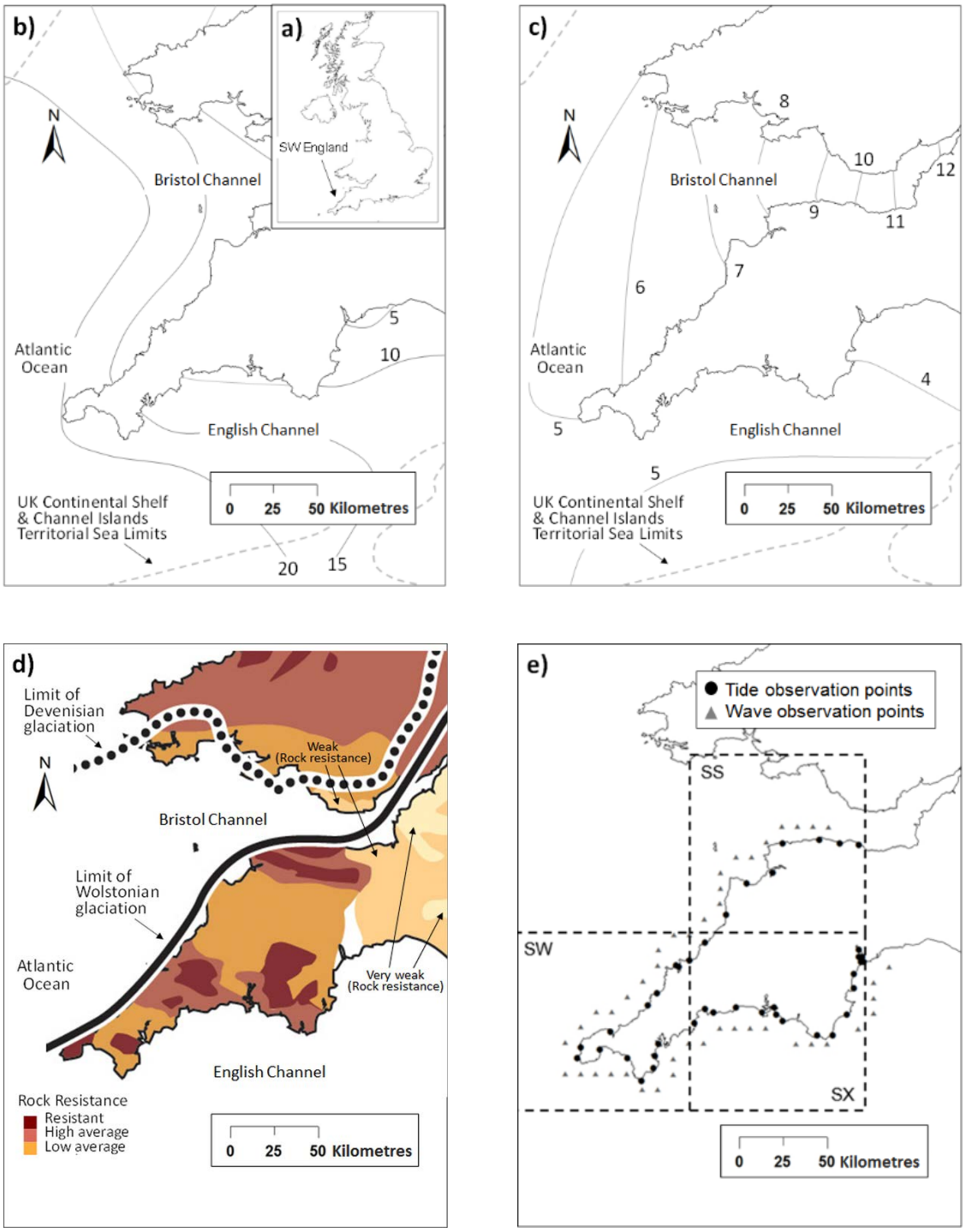

Fig. 1. a) Map of the England; b) mean wave power, based on hourly model hindcast over 7 years, modified from Scott et al. (2011); c) mean spring tidal range (based on data derived from an average tidal year), modified from Scott et al. (2011); d) resistance of geology to denudation, modified from Clayton and Shamoon (1998); and e) map of study area with hatched squares showing the location of Ordinance Survey Great Britain 1936 (OSGB36) grids in the study area and OSGB36 grid names. Circles and triangular marks in Fig. 1e show locations of points where estimates exist of wave height, mean spring tidal range (MSR) and mean sea level (MSL).

80

81

This study used the “SS”, “SW”, and “SX” tiles from OSGB36 which covers approximately 700 km of coastline from east of Minehead in the north, to east of Exeter in the south (Fig. 1e). Fig. 1e also shows the locations of points where tide and wave data used in this study were observed/estimated.

3. Methods

Algorithms were developed to allow (1) semi-automatic extraction of shore platform cross-shore profiles from digital elevation models, and (2) morphometric analysis.

3.1. LiDAR-derived surface models

A digital elevation model (DEM) derived from LiDAR surveys along England coastline was provided by the Channel Coastal Observatory (http://www.channelcoast.org/). DEMs were captured using an OPTEC GEMINI and OPTEC ALTM 3100 system coupled with a dual frequency carrier phase global navigation satellite system for positioning. Cleaning (e.g., removing spurious points such as flying birds or fog, etc.) and filtering (e.g., removing seawater, building and vegetation) had already been applied to the raw digital surface elevation (Channel Coastal Observatory, 2014). The resulting processed DEMs were provided as a form of 1000 m or 500 m square tile on the OSGB36 grid, with 1 m spatial resolution containing either 1000 x 1000 or 500 x 500 elevation values, referenced to the Ordnance Datum Newlyn with minimum vertical accuracy of ± 0.1 m. This was achieved through ground-truthing using hard surface and/or features with known elevation, surveyed using real time kinematic (RTK) global positioning system which yields vertical accuracy of ± 0.03 m, which took place every 10-15 km alongshore distance (Channel Coastal Observatory, 2014).

3.2. Data mining

The Channel Coastal Observatory provided shore-normal transect lines at approximately 50 m intervals around the southwest England shoreline. These transects are ideal locations to extract elevation data from the DEMs, because most of the transects have an accompanying shoreline classification, such as: rock platform, beach, rock platform with beach, and various engineering features (e.g. groynes, breakwaters). Table 1 shows a general breakdown of transect categorization in the currently studying

area. Our analysis focussed on the rock (shore) platform categorisation; transects were omitted if they were categorized other than 'Rock Platform' or 'Cliff-Rock Platform', or had no categorisation, more than one categorisation, or engineering features. As a result, 6,764 transect lines were obtained as potentially useful shore platform transects (Table 1)

Table 1. Breakdown of the number of shoreline types along the southwest England coastline.

Shoreline classification	Type	Number of transects	Ratio
Natural features	Cliff / Cliff with others such as beach	3,758	28.2%
	Cliff-Rock Platform / Rock Platform	**6,764**	**50.8%**
	Beach (including barrier / shingle beach)	386	2.9%
	Dune / Inter-tidal / Spit / Inlet Entrance	75	0.6%
Natural features plus coastal defences	Cliff/Rock Platform - Rock Revetment/Seawall	282	2.1%
	Beach-Embankment/Revetment/Seawall/Groyn	457	3.4%
Coastal defences	Breakwater / Embankment / Revetment / Seawall	105	0.2%
No or more than one categorization		1,489	11.2%
Total		13,316	100%

Each transect line was extended 1.2 km in length to ensure that it encompassed the seaward and landward extent of the landform of interest. Some transects were found to deviate significantly from the shore-normal orientation of the coast, particularly where the coastline was rugged in planform. These profiles were excluded by estimating the average shoreline bearing for each transect (on the basis of the crossing points between shoreline and the two adjacent transects) and eliminating transects if $D < 60°$ or $D > 120°$, where D ($0° <= D <= 180°$) was the angle between the transect and the average shoreline bearing (Fig. 2). As a result, 1,223 transects out of potentially useful 6,764 transects were excluded.

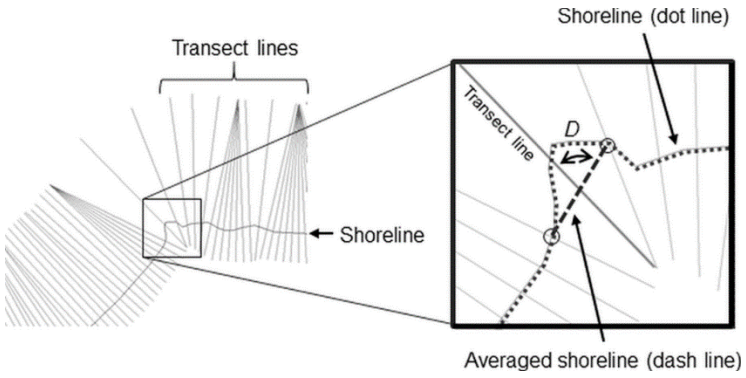

Fig. 2. Schematic view of piece-wise averaged shoreline for each transect.

125

126 Fig. 3 shows a process flow of the profile-extraction methodology. DEMs, shore-normal transects and
127 shoreline types were manually downloaded from the Channel Coastal Observatory. Computer programs
128 were developed to automatically store coordinate information of DEMs in a look-up table (LUT) and
129 extract cross-shore profile elevation data. For each transect, the corresponding DEM(s) was(were)
130 retrieved using a look-up table, and transect orientation and shoreline type were examined to select
131 "true" shore-normal shore platform transects. Elevation values were estimated at 1 m spacing across
132 transects by interpolating the values of the DEM cell within which each sampling point occurred, and
133 in the eight surrounding DEM cells (Fig. 4).

134

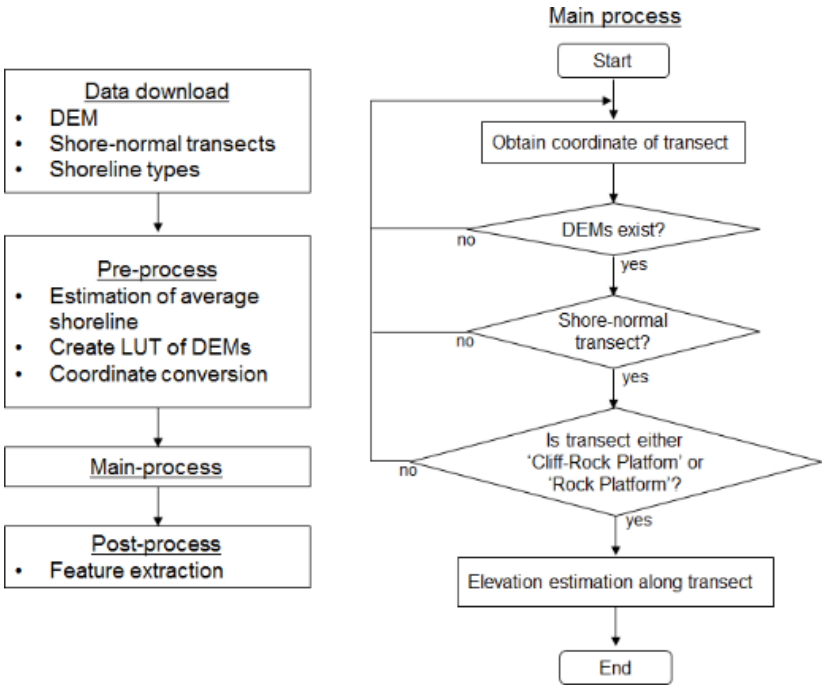

Fig. 3. Overview of semi-automated shore platform profile extraction.

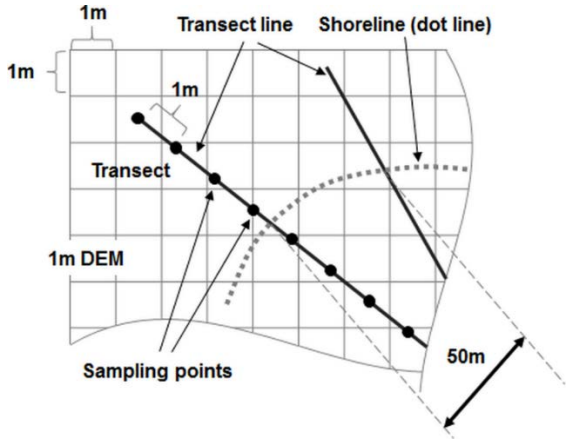

Fig. 4. Schematic view of cross-shore profile extraction from 1 m DEM. The horizontal and vertical coordinates of each sampling point are rounded off to the closest first decimal number in order to uniquely determine the elevation value.

3.3. Morphometric description

Many different aspects of meso-scale shore platform morphology have been described in the research literature (e.g. see Trenhaile, 1987), and more recently there has been focus on micro-scale morphological descriptions (e.g. Dornbusch et al., 2008; Dornbusch and Robinson, 2011). For this study we focussed on automatically characterising meso-scale morphology; the mean intertidal platform gradient (PG), intertidal platform width (PW) and intertidal platform roughness (PR). These metrics were determined for each cross-shore platform profile using three equations (Eq. (1)-(3)), where N is the total number of sampling elements along the transect, and F is an approximate line extending between mean high water spring (MHWS) and mean low water spring (MLWS) elevations. Shore platform roughness was estimated by analysing the variability in a polynomial regression line fitted through sampling points between MHWS and MLWS. The order of the polynomial regression line used in analysis was selected by systematically increasing the order (1, 2, 3…) and examining roughness values. The mean and standard deviation of roughness values decreased as the order of the polynomial

regression increased, but almost no difference in mean and standard deviation of roughness values was detected above 6th order; hence, a 6th order polynomial line was selected for the purpose of estimating platform roughness.

$$PG = \tan^{-1}\left((Z_{MHWS} - Z_{MLWS} / X_{MHWS} - X_{MLWS}\right) \quad \text{Eq. (1)}$$

$$PW = X_{MHWS} - X_{MLWS} \quad \text{Eq. (2)}$$

$$PR = \sqrt{\sum_i \left(Z_i - F_i\right)^2 / N} \quad \text{Eq. (3)}$$

Positions on the profile of the MHWS and MLWS tidal levels were calculated by linearly interpolating their elevation, as shown in Fig. 5. Morphometric estimations were excluded when there were no elevation points extending up to MHWS or down to MLWS. Owing to across-shore profile variation in platform morphology, some profiles had more than one MHWS or MLWS elevation intersection. In these cases the seaward-most MWHS and MLWS positions of profiles which extended up to and down to MHWS and MLWS were selected for morphometric calculations. Shore platform profiles sometimes exhibit across-shore curvature with more steep and gentle slopes at higher and lower intertidal elevations (e.g. Trenhaile, 1974; Blanco-Chao et al., 2003). For this reason, PG, PW, and PR were also evaluated for upper, lower, and central intertidal profiles, as described in Table 2. Describing PG and PW requires identification of the outer (seaward) margin of the shore platform. Kennedy (2015) has described the difficulties faced with field researchers making this decision. We defined the outer margin as the seaward point on a profile corresponding with MLWS elevation, because in the absence of field-survey, a repeatable classification method was necessary.

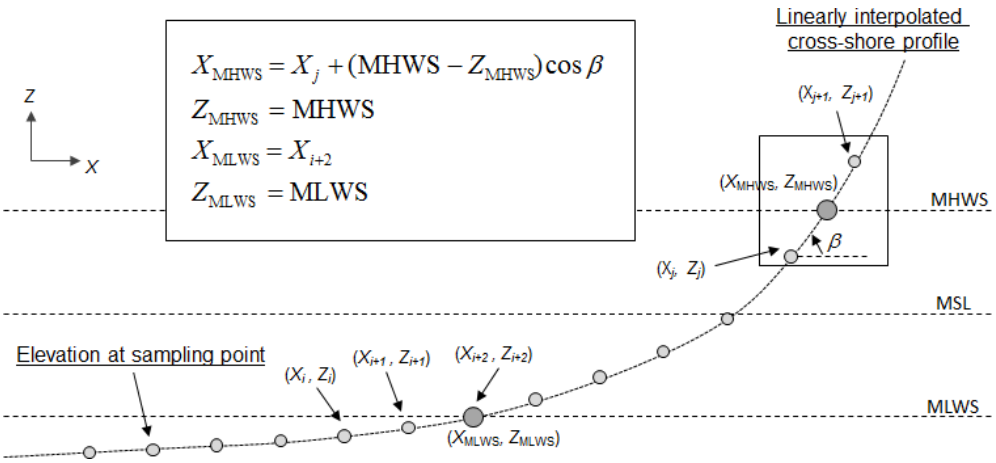

Fig. 5. Cross-sectional view of a profile with positions at MHWS and MLWS.

Table 2. Upper and lower limit of profile elevation of whole, upper, lower, and central intertidal profiles.

	Whole	**Upper**	**Lower**	**Central**
Upper limit of profile elevation	MHWS	MHWS	MSL	MSL+MSR/4
Lower limit of profile elevation	MLWS	MSL	MLWS	MSL-MSR/4

3.4. Process-regime description

The MSR and MSL were estimated for each transect by linearly extrapolating observed MSR and MSL at two points with exact coordinates to the nearest transect line, obtained from Admiralty Tide Tables (2016) (Fig. 6). Mean wave height variations for each transect were estimated in a similar way, using modelled data provided by the UK Met Office (representing waves in 20–30 m water depth and obtained from their 8 km grid model) for the 2011-2013 period along the southwest coast of England. Nearshore wave transformation was not modelled for this study. Instead, each transect was automatically categorized as exposed, partly-exposed, partly-sheltered or sheltered, depending on the relative orientation between the transect (from seaward to landward) and the prevailing WSW wave direction in the study area (α). To obtain the nearshore wave height, the modelled 'deep water' wave height was simply multiplied by a multiplier *K*, depending on α: $K = 1$ for $0° <= |\alpha| < 45°$; $K = 0.75$ for $45° <= |\alpha| < 90°$;

187 K = 0.5 for 90°<=|α|<135°; K = 0.25 for 135°<=|α|<180°) (Fig. 7). Detailed geological information was
188 not available for each transect. Instead, the work of Clayton and Shamoon (1998) was used to manually
189 locate the coordinates of boundary points that divide geological areas of 'high' rock strength, 'high
190 average', and 'low average', with values of 100, 10, and 1MPa, respectively, assigned to these
191 categories.
192

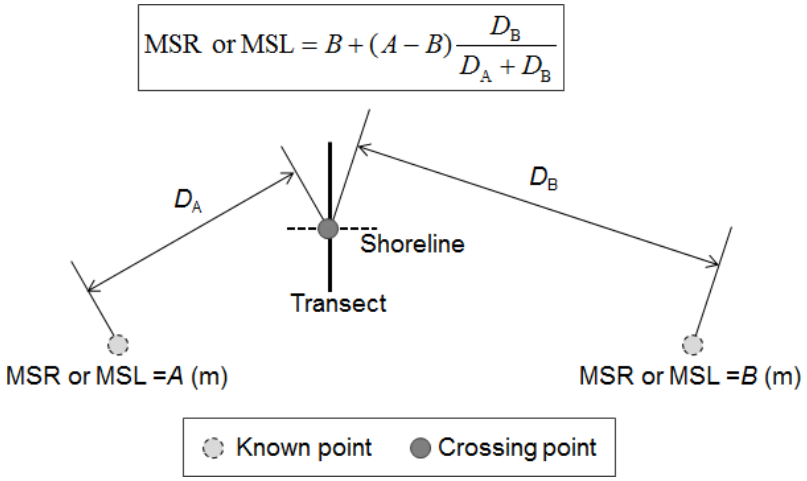

Fig. 6. Relative position of MSR/MSL-known points and crossing point with average shoreline and transect.

193
194

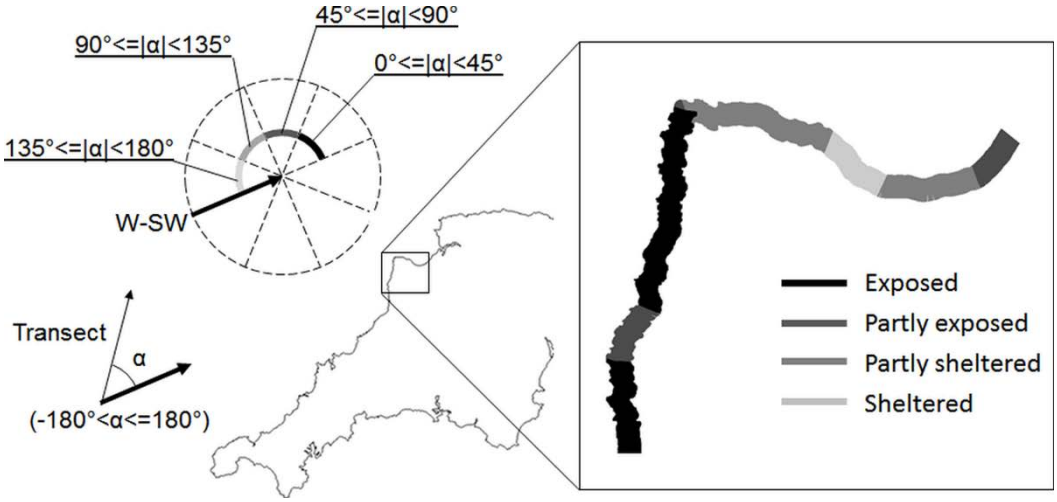

Fig. 7. Transect categorization examples in respect to wave exposure.

195

4. Methodology: development of a semi-automated method for shore platform morphometric description

This section describes a new method for selecting and extracting the morphometric characteristics of shore platform profiles from a large DEM dataset. The method is dependent on the existing shoreline classification provided by the Coastal Channel Observatory. In this classification we believe that some profiles that are mapped as shore platforms (presumably in a desk-top aerial photograph exercise) may in fact be low-slope, but very 'rough' rocky foreshores that might not be typically identified for research investigation by field workers interested in shore platforms. It is important that our study is comparable with the existing shore platform literature. Hence, to examine the comparability of the proposed method, we conducted a preliminary application of the method to selected shore platform sites in southwest England known to the authors.

Two well-recognized shore platform sites in North Devon and Cornwall, shown in Fig. 8, were selected for the 'ground-truthing'. Fig. 9 shows ten consecutive cross-shore profiles for each of the sites with seaward and landward margins. Table 3 shows the average PG/PW/PR values at each site. Of note, non-shore-normal profiles (dot lines) are excluded in the calculations presented in Table 3. Most of the extracted cross-shore profiles exhibit a low-gradient intertidal slope, extending from seaward at around the MLWS elevation to a cliff-platform junction between MSL and MHWS elevations, particularly at Hartland Quay (Fig. 9a). Gradually sloping cross-shore profiles at Porthleven often occur at lower intertidal elevations, and cliff-platform junctions sometimes occur even below MSL, resulting in very steep cliff profiles or narrow ramps/ledges at upper intertidal elevations (Fig. 9b). Examples of very rough intertidal profiles, which vary markedly at intertidal elevations, occur at both sites (e.g. No.2 and No.6 profiles in Hartland Quay and No.6 profile in Porthleven), and should be categorized as non-platform profiles.

Fig. 8. Shore platforms at a) Hartland Quay in North Devon and b) Porthleven in Cornwall (Photos from Google Earth: https://www.google.com/earth/)

222

223

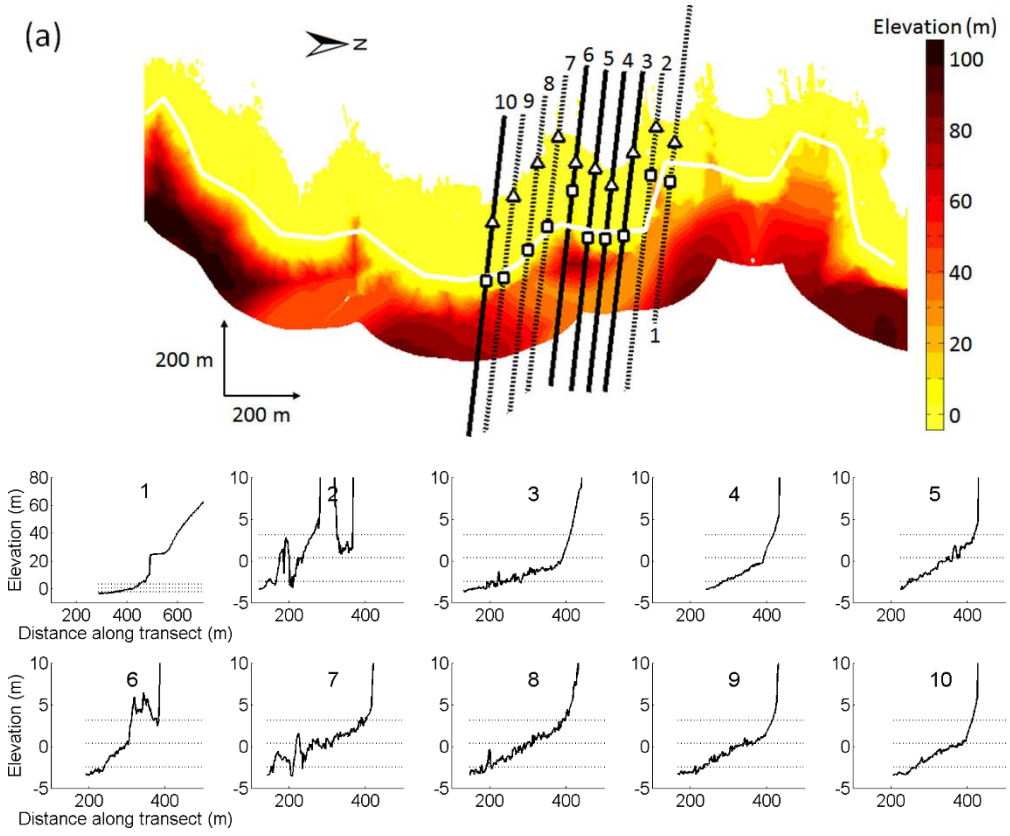

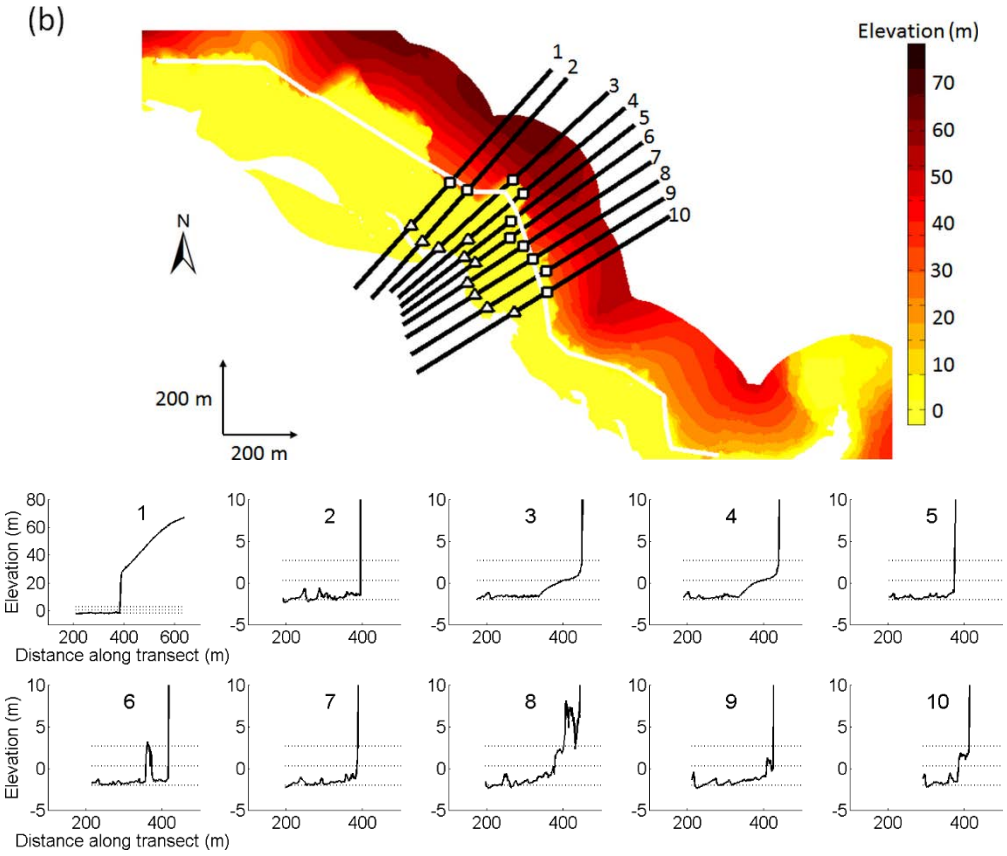

Fig. 9. DEMs with ten consecutive transects (black lines) and shoreline (white lines) and profiles at: (a) Hartland Quay and (b) Porthleven. (1) Seaward and landward margins for each transect are shown as triangles and square marks, (2) dot lines in DEMs show transects with large deviation from averaged shoreline which are removed in the average estimations presented in Table 3, and (3) dot lines in cross-shore profiles indicate MHWS, MSL, and MLWS elevations respectively. Of note, different horizontal and vertical scales are used to show both whole cross-shore (transect 1) and intertidal cross-shore profiles (transects 2-10).

224

225

Table 3. Summary of average intertidal profile characteristics of shore-platform transects in Hartland Quay - North Devon and Porthleven. Note that average calculation only considers 'shore-normal' profiles (excluding dot lines).

	North Devon			Porthleven		
	PG [degrees]	PW [metres]	PR	PG [degrees]	PW [metres]	PR
Whole	2.5	146	0.18	1.6	174	0.27
Upper	6.3	36	0.11	32.0	17	0.08
Central	2.6	69	0.12	16.8	80	0.15
Lower	1.7	110	0.13	0.9	158	0.18

226

The average PG of the whole, central and lower intertidal profiles at Hartland Quay is between 1.7 and 2.6°, whereas the upper intertidal profile slopes at 6.3° on average, because of the influence of a steeper gravel/boulder beach at the site (Table 3 and Fig. 8a). At Porthleven the PG of the lower intertidal profiles is less than 1 degree, whereas the cross-shore profile slopes steeply in upper and central portions (32.0° and 16.8° respectively), due to the presence of the cliff face at upper intertidal elevations (Fig. 9b). The average PR at both sites is highest for the whole intertidal profile and lowest for the upper intertidal section, but there is no clear consistency in PRs found between the two sites (PRs at different elevations were almost consistent in North Devon whereas there was an increasing trend of PR with the elevation at Porthleven). It should also be noted that most of the PR values exceed the minimum vertical accuracy of the DEMs used in this study. Hence, the roughness estimates are unreliable and cannot be used to inform observations of micro-surface morphology (e.g. see Dornbusch et al., 2008; Dornbusch and Robinson, 2011).

Initial ground truthing revealed that calculations using profile points at particular tidal levels (e.g. MSL, MHWS) occasionally resulted in inappropriate estimates of shore platform features; for instance, due to the presence of non-shore platform features such as gravel/boulder beaches, steep cliffs or ramps/ledges at upper intertidal elevations. To appropriately extract shore platform profiles, we developed a method to automatically identify the cliff-platform junction (CP) and subsequently characterize the shore platform morphology by analysing the section of profile extending between CP and the seaward-most point (SP) corresponding with MLWS. Several conditions were used to find the CP in relation to some SP and a landward point (LP) on the profile. (1) The width between CP and SP and the gradient of the CP-SP slope were set as > 100 m and < 10^{o}, respectively, so that the CP occurs at a wide range of elevations, without tidal elevational constraints, up to about 17 m (~ $\tan 10^{o}$ x 100 m) above MLWS. (2) The height and the gradient of CP-LP slope was set as > 3 m and > 45^{o}, respectively, as we focused on shore platforms backed by a moderately higher and steeper cliff. Of note, the search for the LP was conducted up to 3 m horizontal distance from CP due to computational efficacy. The resulting CPs were often found at elevations above higher intertidal elevations, even with the possible occurrence of high tide beaches in profiles. To remove the possible effect of beaches at higher intertidal

255 elevations, a landward-most point at MSL (CP-MSL) was used as the CP when (1) CP elevation was
256 higher than MSL or (2) CP-LP slope was > 5^{o} assuming that CP-LP slope was non-shore platform slope
257 (< 5^{o}). When all CP/CP-MSL, SP, and LP were found, PG, PW, and PR were estimated using a profile
258 extending between CP/CP-MSL and SP.
259
260 In total 612 transects out of possible 5541 transects (11%) were identified as shore-normal shore
261 platform profiles with clear cliff-platform junctions. A large reduction of possibly useful shore platform
262 profiles occurred because the CPs occur in a variety of geometric conditions in nature, whereas the CP-
263 search was conducted automatically with a fixed geometric rule. We also verified the modified method
264 by manually checking all the profiles, and confirmed that the selected 612 profiles and their SP and CP
265 locations were sensible. For example, possible high tide beaches at higher intertidal elevations in No.4
266 and No.10 profiles from Hartland Quay were removed with the automated method, whereas the CP
267 below MSL in No.1 and No.4 profiles from Porthleven were appropriately selected (Fig. 10).
268

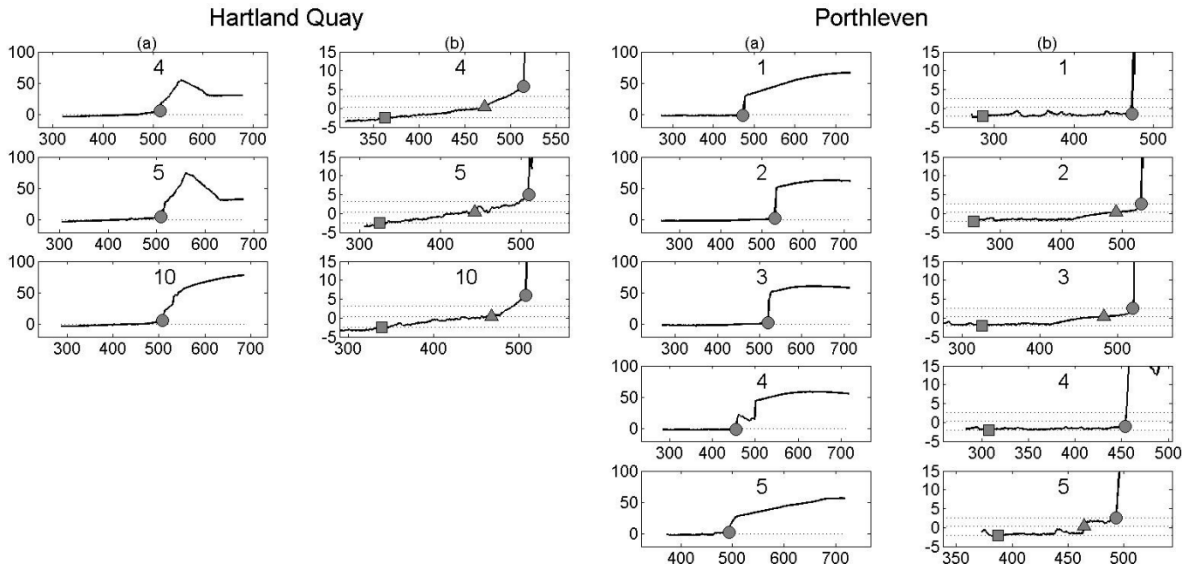

Fig. 10. Selected profiles from Hartland Quay and Porthleven: (a) whole profile and (b) intertidal profile. Number in each figure matches with those used in Figure 9. Circle, square, and triangle markers represent CP, SP and CP-MSL, respectively. Of note, (1) CP-MSL is not shown when slopes between CP and SP slope are used in calculation, (2) horizontal and vertical axis represent distance along transect in metres and elevation in metres, and (3) dot lines in intertidal profiles indicate MHWS, MSL, and MLWS elevations.

269

5. Results

This section examines the morphology of 612 shore platform profiles identified around the southwest coast of England in respect to geographical location and possible environmental controls on morphological development.

5.1. Region-wide comparison of shore platform morphology

The estimated PG, PW, and PR of the selected 612 shore platform profiles along about 700 km of coastline from north to south are plotted in Fig. 11. We further divided the coastline into ten even segments and plotted the mean and standard deviation of each segment. The trend lines were estimated based on a linear regression analysis using the mean values of the segments.

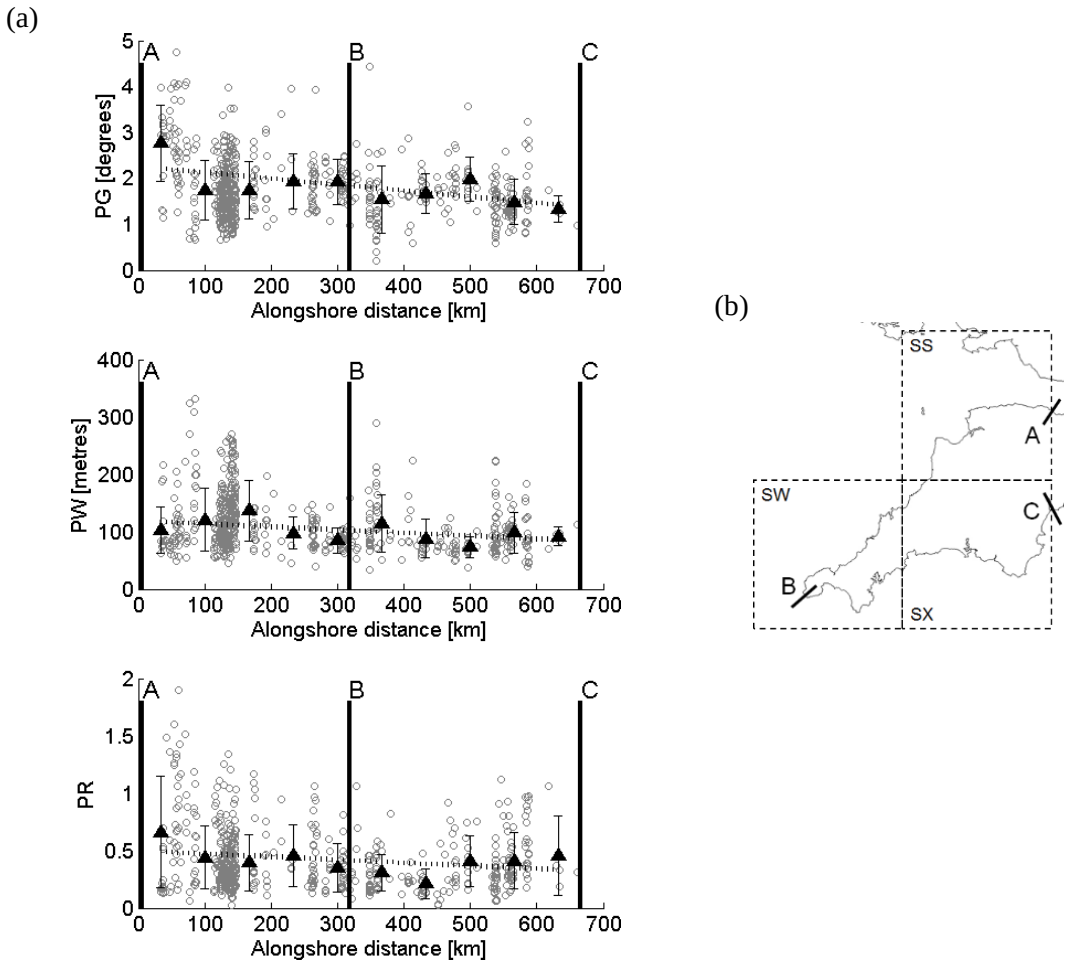

Fig. 11. (a) PG, PW and PR of shore platform profiles in SW England. Triangle markers and their error bars show mean values and standard deviations of all the data in each even

segment, and dots lines show linear trend lines. (b) A map of south west England with area lines indicating the relative position of A, B and C.

Results are scattered, and the standard deviation is high, but there are general region-wide trends observed in shore platform morphology. For example, there is a gradual decreasing alongshore trend in PG from the north (line A) to south-west (line B) and south-east (line C). A similar decreasing trend is apparent both in PW and PR, although the trend is less clear, particularly with PR contrastingly increasing from south-west (B) to south-east (C). In very general terms, the data indicate that from north (A) to south-west (B) and south-east (C), shore platforms become flatter, narrower, and smoother. Some clustering of data points is apparent in Fig. 11, particularly between 100-150 km distance alongshore. Testing confirms that when those points are omitted the same decreasing PG/PW/PR trends still occur.

5.2. Correlation with environmental conditions

Statistical analyses were undertaken to explore potential relationships between shore platform morphology and MSR, wave height and rock strength. It is important to note at the outset that the quality of data available for these analyses varies: the estimate of MSR and MSL for each transect is relatively reliable, whereas only offshore wave conditions and transect orientations were considered to estimate nearshore wave conditions, and rock strength data are coarse with no account taken of local structural controls (e.g., strike, dip, thickness of beds, and fracturing). Fig. 12 presents scatter plots and box plots of PG/PW/PR calculated across the shore platform profiles, in relation to MSR, wave height and rock strength; trend lines calculated using a linear regression analysis and correlation coefficients, and p-values calculated using an analysis of variance (ANOVA) are also reported in the same figure.

Trends exist between platform morphology and the different potential process controls (MSR, wave height and rock strength). However, there is considerable scatter and correlation coefficients are generally around 0.3 or less. As Fig. 12 shows, many relationships have very small p-values, implying statistical significance (e.g. PG-MSR relation), but significance should be interpreted cautiously given that there is a low degree of correlation, and that p values are influenced strongly by large sample sizes.

Overall, however, there are interesting trends in the relations investigated. For example, PG increases with both MSR and rock strength. This relationship is also demonstrated by the box plots, although it is notable that, when grouped, increases in MSR/rock strength result in a stepped rather than regular increase in PG, raising the possibility of threshold effects (for instance, compare box-plots above and below 7 m MSR and 10 MPa or below and 100 MPa rock strength). In contrast, a negative decreasing trend was detected between PG and wave height. Generally, the data indicate that flatter platforms occur where the tidal range is smaller, rock strength is weaker, and where there are larger waves. The PW trend line also increases with MSR, but in contrast to PG, it increases with wave height and decreases with rock strength. These results are physically sensible (e.g. wider platforms occur where waves are bigger, tidal range is larger, and rocks are weaker), and exists despite difficulties associated with usefully measuring PW. For instance, PW in some instances is calculated as the horizontal distance between SP and CP, but in other instances, it is the horizontal distance between SP and CP-MSL (e.g. when possible high tide beach profiles occur). PR increases with MSR and rock strength, in contrast to a negative trend between PR and wave height. Correlation coefficients and p-values are smaller and larger, respectively, in the PR-related relations, but, again in a broad view, there is physical sense to the direction of trends: rougher platforms occur where there are harder rocks, smaller waves and larger tidal ranges (because wave attack operates for less time across a larger band of rocks).

(a)

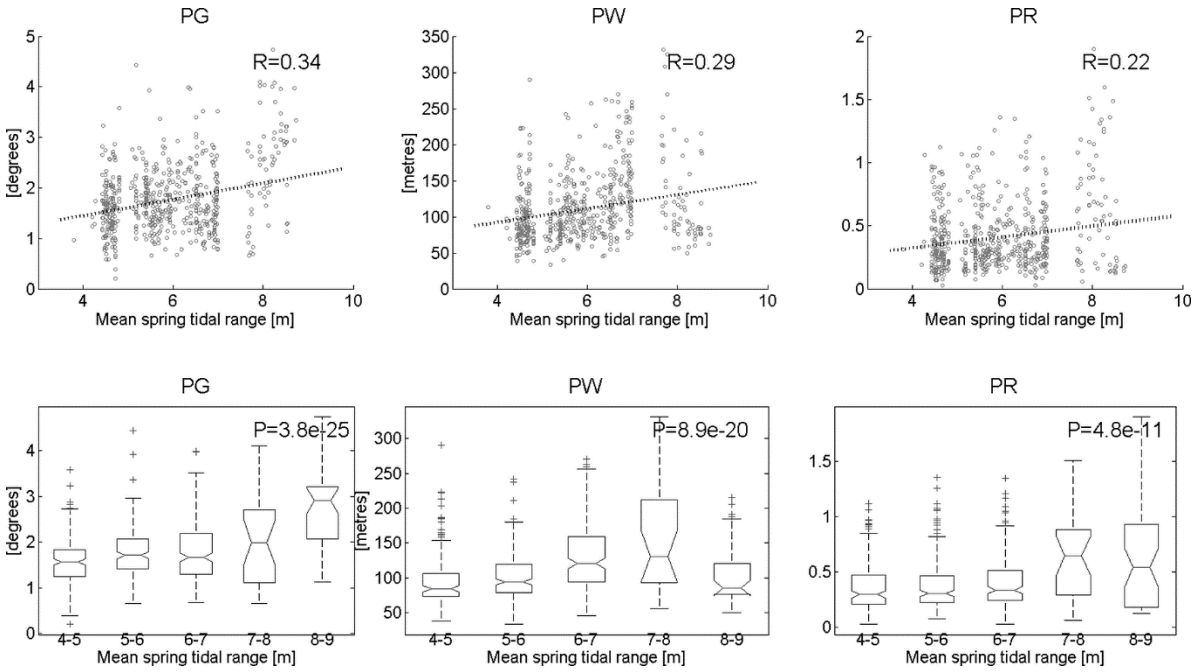
PG
R=0.34
[degrees]
Mean spring tidal range [m]
PW
R=0.29
[metres]
Mean spring tidal range [m]
PR
R=0.22
Mean spring tidal range [m]
PG
P=3.8e-25
[degrees]
4-5
5-6
6-7
7-8
8-9
Mean spring tidal range [m]
PW
P=8.9e-20
[metres]
Mean spring tidal range [m]
PR
P=4.8e-11
Mean spring tidal range [m]

(b)

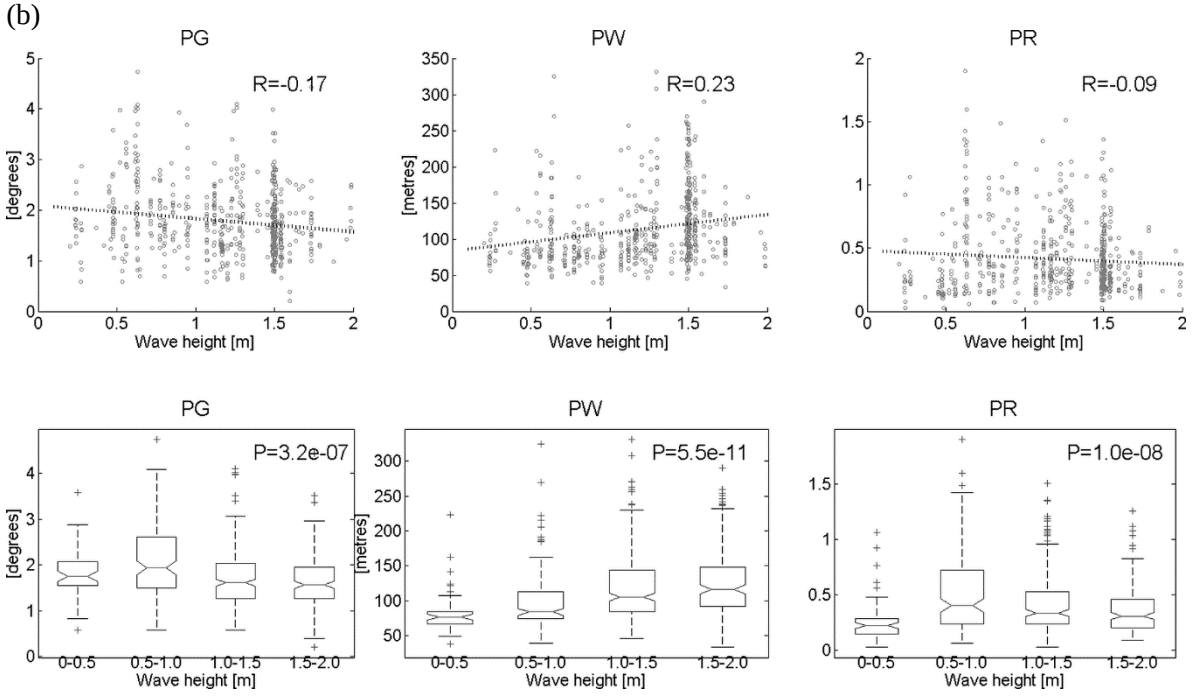
PG
R=-0.17
[degrees]
Wave height [m]
PW
R=0.23
[metres]
Wave height [m]
PR
R=-0.09
Wave height [m]
PG
P=3.2e-07
[degrees]
0-0.5
0.5-1.0
1.0-1.5
1.5-2.0
Wave height [m]
PW
P=5.5e-11
[metres]
Wave height [m]
PR
P=1.0e-08
Wave height [m]

(c)

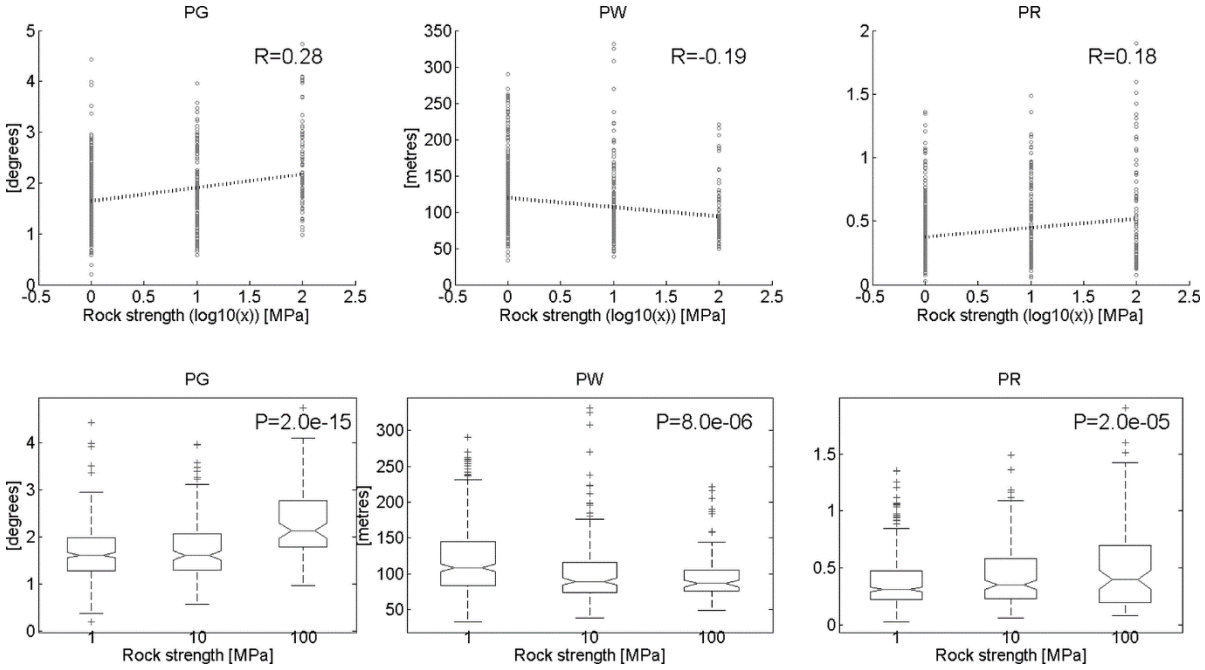

Fig. 12. Scatter plots and box plots of PG, PW and PR of shore platform profiles in relation to: (a) MSR, (b) wave height and (c) rock strength. Correlations coefficients (R) and p-values (P) are reported at the top-right of each scatter and box plot. Dot lines represent trend lines drawn from a liner regression analysis. Box plot shows median values (mid lines in the boxes), 25 and 75 percentile values (box outline), minimum and maximum values excluding outliners (whiskers), and 1.5 interquartile range (IQR) outliers (plus markers).

6. Discussion

The results from this paper demonstrate that LiDAR-derived DEMs can be used to systematically extract and analyse shore platform morphology at regional scales (i.e. hundreds of kilometres). This is a new spatial scale of analysis in rocky shore studies; the vast majority of previous work has focussed on descriptions of profile morphology across hundreds of metres to tens of kilometres at discrete field sites. The discussion below (1) considers process controls on shore platform development in the study area (~700 km of coast in southwest England), (2) describes a new simple empirical model describing shore platform gradient, and (3) examines the potential broader applicability of the method described in this paper for studies of rocky shore geomorphology.

6.1. Process controls on shore platform morphology

Previous field and modelling studies have suggested associations between platform morphology (e.g. PG, PW, PR) and various aspects of the process environment (Table 4). Perhaps the most widely known of these is a general positive correlation noted in field surveys by Trenhaile (1972, 1974, 1987, 1999) between PG and MSR. In addition, positive correlations have been noted between PG and rock strength (e.g. Trenhaile, 2005), PW and MSR (e.g., Trenhaile and Layzell, 1981; Trenhaile, 2000, 2005), and PW and wave intensity (e.g., Sunamura, 1978; Trenhaile, 1999, 2005). Trenhaile (2005) also showed that PG decreases with PR, which indirectly suggests a positive correlation between PR and MSR.

Table 4. Examples of previous studies regarding environmental controls on platform morphology and the trends in this study

Shore platform morphology	Process	Trend observed in this study	Trend found in previous study	Reference	Study type
PG	MSR	Positive	Positive	Trenhaile (1972, 1974, 1987,1999)	Field observations
	Rock strength	Positive	Positive	Trenhaile (2005)	Modelling study
PW	MSR	Positive	Positive	Trenhaile and Layzell (1981), Trenhaile (2000, 2005)	Modelling study
	Wave intensity	Positive	Positive	Sunamura (1978), Trenhaile (2005)	Modelling study
		Positive	Positive	Trenhaile (1999)	Field observations
PR	MSR	Positive	Positive	Trenhaile (2005)	Modelling study

Direct quantitative comparison of the trends observed in field studies with those found in this study is difficult, owing to different classification and description methods. However, the overall qualitative consistency between previous findings and our systematic and automated analysis of LiDAR data is noteworthy. The results are also somewhat surprising (in the sense that trends exist at all) because: (1) there are many potential sources of variability that exist from transect to transect; and (2) we have only taken very approximate representations of the process environment at each site.

Observed relationships between shore platform morphology and controlling processes (i.e. MSR, wave height, and rock strength) exhibit considerable scatter (Fig. 12), and caution needs to be exercised in any attempt to link correlation with causation. It is unsurprising that scatter exists given the approximate way in which environmental conditions were estimated at each transect. For example, offshore wave conditions mediated by shoreline orientation were used to estimate nearshore wave conditions, whereas complex transformations in wave energy are known to occur as waves transform inshore toward each transect, and these are not fully accounted for in our analysis. Our analysis also neglects any possible formative role for storm waves, which have been linked to erosion on many rocky coasts (e.g. Bartrum, 1926; Edwards, 1941, 1951; Cotton, 1963; Sunamura, 1978; Trenhaile, 1980) including the southwest of England (Earlie et al., 2015). Further, Trenhaile (1987) highlighted that in nature sometimes opposite trends occur between platform morphology and the expected environmental control owing to factors such as local variability in rock structure (e.g. bedding orientation, joint density, presence/absence of faults, etc.) which can be locally dominant (e.g. Trenhaile, 1972; Dickson et al., 2004; Naylor and Stephenson, 2010; Cruslock et al., 2012; Moses, 2014). It is evident that local rock structure in the studied coasts is highly varied (e.g., May, 1980) and must account for a least some of the scatter in the results.

Inheritance of platform morphology from previous sea-level positions can also result in unusual relationships between platform morphology and various aspects of the process environment. For example, Bird and Dent (1966) noted that in southeast Australia, wider shore platforms sometimes occur in more sheltered embayments. Brooke et al. (1994) showed that some platforms on this coast are inherited from previous sea-level highstands, and that these inherited platforms are sometimes wider in sheltered environments as they have suffered less erosion of their seaward edge during the present sea-level highstand. The role of inheritance in shaping the geomorphology of contemporary shore platforms in the southwest of England is not clear; however, there is an abundance of evidence for the presence of raised shore platforms from previous inter-glacial period(s) (Orme, 1960). These highstand platforms ‘merge’ with the contemporary platforms and this may have contributed additional scatter to the correlations observed in this study.

Factors such as varied rock resistance and inheritance lead Mii (1962) to conclude that shore platform morphology is a very ambiguous indicator of process. This statement has often been repeated (e.g. Stephenson 2000). We have not attempted to account for complex potential sources of uncertainty in our analysis, so the fact that trends can be seen between platform morphology and various indicators of the process environment likely stems from the large spatial scale of analysis. For example, despite the overall consistency, there are many local inconsistent trends seen in Fig. 11. It appears therefore that selectively but systematically observing morphology over a large spatial area, encompassing a wide range of forcing processes, it is possible to observe the general nature of process-form dependency.

The present study illustrates that shore platform morphology is dependent on multiple controls: all of the three controls we analysed had some association to platform morphology, and there will be other controls that we did not study that are likely to be important as well (e.g. storm waves, weathering processes, inheritance from former sea-level positions). Below we describe a simple empirical model to describe shore platform gradient based on the three controls studied in this paper.

6.2 Empirical model of shore platform gradient

Several empirical models exist describing shore platform morphology, including the wave erosion models of Tsujimoto (1987) and Sunamura (1992), which demarcates the development of sloping type-A and sub-horizontal type-B shore platforms in relation to the relative forces of wave erosion and rock strength. Here we examine the empirical model of Trenhaile (e.g. 1999), which predicts mean PG in relation to MSR. The field data included in Trenhaile's (1999) analysis cover a wide spectrum of tidal regimes from micro to mega tides. A strong correlation exists between PG and MSR across the entire MSR space, although scatter in the data mean that this correlation would not be obvious if analyses were conducted across a narrow tidal range (see Fig. 2 in Trenhaile, 1999).. An improved model of PG for these data might benefit from consideration of additional environmental controls (beyond MSR). To examine this possibility, single- and multi-linear regression analyses were undertaken, considering MSR, wave height and rock strength assuming no co-correlation among independent variables.

411

412 Equation 4 and 5 provide models of PG with no intercept, similar to the empirical model by Trenhaile
413 (e.g. 1999), where X_1, X_2 and X_3 represent MSR in metres, wave height in metres, and rock strength in
414 MPa. Table 5 shows statistical summaries of the single- and multi-linear regression analysis with an
415 ANOVA analysis, and Table 6 compares root mean square errors (RMSE) of PG models including
416 Trenhaile's (1999) with respect to field data from Trenhaile (1999) and SW UK using LiDAR DEMs.

417

418 $$PG_{\text{single}} = 0.30X_1 \quad \text{Eq. (4)}$$

419 $$PG_{\text{multi}} = 0.31X_1 - 0.13X_2 + 0.19\log10(X_3) \quad \text{Eq. (5)}$$

420

Table 5. Statistical summary of single- and multi-linear regression analysis (left) and ANOVA analysis.

		Estimated coefficients					**Anova**				
		Estimate	Standard Error	tStat	pValue		SumSq	DF	MeanSq	F	pValue
						Total	332.4	612	0.54		
PG_{single}	X_1	0.30	0.01	68.13	1.4e-289	Model	72.9	1	72.93	172.05	8.1e-35
						Residual	259.4	611	0.42		
	X_1	0.31	0.01	22.81	9.3e-84	Total	341.9	612	0.56		
PG_{multi}	X_2	-0.13	0.06	-2.20	2.8e-02	Model	98.7	3	32.89	82.66	7.0e-45
	X_3	0.19	0.04	5.27	1.9e-07	Residual	242.7	610	0.40		

421

Table 6. RMSE of various models using field data from Trenhaile (1999) and SW UK (LiDAR DEMs). Bold values represent RMSEs of single-factor best fit linear models, and values in the brackets show percent deviation relative to the RMSE of single-factor best fit linear models.

	Data from Trenhaile (1999)	Data from SW UK using LiDAR DEMs
Trenhaile's model (PG=0.26X_1)	**0.59**	0.70 (+10%)
PG_{single}	0.67 (+13%)	**0.65**
PG_{multi}	-	0.62 (-5%)

422

Table 5 shows that the estimated coefficients and the models themselves are significant at 5% significance level (p-values < 0.05). More importantly, Table 6 shows that, although PG_{single} fits better with SW UK data (smaller RMSE compared to the equation provided by Trenhaile, 1999), PG_{multi} further reduces the RMSE of PG_{single} by 5%. A 5% reduction in RMSE is not particularly large, but this is not at all unexpected given the coarse estimates of wave height and rock strength used. Our expectation is that improved estimates (measurements and/or modelling) of a range of environmental controls, coupled with large-scale morphometric analyses, would achieve better quantitative understanding of the relative importance of different controls on rocky coast morphology development.

7. Conclusions

This study describes a new semi-automatic method for analysing shore platform morphology over large spatial scales using LiDAR-derived surface elevation models. DEMs with 1 m spatial resolution and 0.1 m RMSE are sufficiently detailed to enable algorithmic calculation of shore platform gradient and platform width (but not platform roughness). Our results from 700 km of coast in southwest England are broadly consistent with previous field studies undertaken at a relatively small number of selected sites in which it has been shown that shore platform gradient is positively correlated with tidal range. In addition, we find that shore platform gradient varies with wave height and lithology and conclude that in southwest England, shore platform gradient is best predicted using an empirical model that considers tidal range, wave height and rock strength. There is considerable scatter in the relationships but this is not surprising given the extent of local variability that exists along the coast, and the very coarse way that process controls have been represented in our study (particularly wave height and rock strength). Rocky shore geomorphology is known to be influenced by many factors that we have not considered (e.g. storm waves, local geological discontinuities, morphological inheritance from previous sea-level positions, etc.). In this regard it is encouraging that general relationships can be seen between shore platform geometry and metrics of tidal regime, wave climate and geology. We conclude that this is likely attributable to the very large scale of analysis conducted. Given the widespread availability of high resolution coastal DEMs, it should be possible to conduct even larger scale analyses of rocky shore landforms and formative environmental controls, particularly if it is possible to combine such analyses

with more detailed information (modelled or field) relating to process-controls, such as nearshore wave energy and geological/lithological/structural variability. In this way, large-scale analysis of coastal DEMs might address the call from Naylor et al. (2010) for rocky shore evolution models to improve calibration of model coefficients using field data.

Acknowledgments

Mark Dickson was part-funded by the MBIE funded Natural Hazards Research Platform through Contract C05X0907 ("Climate change impacts on weather-related hazards"). Gerd Masselink was part-funded by EPSRC grant Waves Across Shore Platforms (WASP; EP/L025191/1).

References

Adams, P. N., Anderson, R, S., Revenaugh, J., 2002. Microseismic measurement of wave-energy delivery to a rocky coast, Geology, 30, 895–898.

Bartrum, J.A., 1926. Abnormal shore platforms. Journal of Geology 34, 793–807.

Bartrum, J.A., 1938. Shore platforms. Journal of Geomorphology 13, 266–272.

Bird, E. C. F.; Dent, O. F., 1966: Shore platforms on the south coast of New South Wales. Aust. Geogr. 10, 71-80.

Blanco-Chao, R., Costa Casais, M., Martínez Cortizas, A., Pérez Alberti, A., Trenhaile, A.S., 2003. Evolution and inheritance of a rock coast: western Galicia, northwestern Spain. Earth Surf. Process. Landf. 28, 757–775.

Brooke, B. P., Young, R. W., Bryant, E. A., Murray-Wallace, C. V., Price, D. M. 1994. A Pleistocene origin for shore platforms along the northern Illawarra coast, New South Wales. Australian Geographer, 25, 178–185.

Channel Coastal Observatory, 2014. Specification of LiDAR surveys. (http://www.channelcoast.org/national/procurement/Specification_Lidar.pdf)

Clayton, K., Shamoon, N., 1998. A new approach to the relief of Great Britain II. A classification of rocks based on relative resistance to denudation. Geomorphology 25, 155-171.

Cotton, C.A., 1963. Levels of planation of marine benches. Zeitschrift Für Geomorphologie, 7, 97–111.

Cruslock, E.M., Naylor, L.A., Foote, Y.L., Swantesson, J.O.H., 2010. Geomophologic equifinality: A comparison between shore platforms in Höga Kusten and Fårö, Sweden and the Vale of Glamorgan, South Wales, UK, Geomorphology 114, 78-88.

Dana, J.D., 1849. Report of the United States exploration 1838-1842. Volume 10, 442.

Dickson, M.E., 2004. The development of talus slopes around Lord Howe Island and implications for the history of island planation. Australian Geographer 35(2), 223-238.

Dickson, M.E., 2006. Shore platform development around Lord Howe Island, southwest Pacific. Geomorphology 76, 295-315.

Dickson, M.E., and Pentney, R., 2012. Micro-seismic measurements of cliff motion under wave impact and implications for the development of near-horizontal shore platforms. Geomorphology 151-152, 27-38.

Dornbusch, U., Moses, C., Robinson, D.A., Williams R., 2008. Soft copy photogrammetry to measure shore platform erosion on decadal timescale. Journal of Coastal Conservation 11(4), 193-200.

Dornbusch, U., Robinson, D.A., 2011. Block removal and step backwearing as erosion processes on rock shore platforms: a preliminary case study of the chalk shore platforms south-east England. Earth Surface Process and Landforms 36, 661-671.

Duperret, A., Raimbault, C., Le Gall, B., Authemayou, C., van Vliet-Lanoe, B., Regard, V., Dromelet, E., Vandycke, S., 2015. High-resolution onshore–offshore morpho-bathymetric records of modern chalk and granitic shore platforms in NW France, Comptes Rendus Geoscience. doi:10.1016/j.crte.2015.06.005

Earlie, C.S., Young, A.P., Masselink, G., Russel, P., 2015. Coastal cliff ground motions and response to extreme storm waves. Geophysical Research Letters 42, 847-854.

Edwards, A.B., 1941. Storm-wave platforms. Journal of Geomorphology 4, 223–236.

Edwards, A.B., 1951. Wave action in shore platform formation. Geological Magazine 88, 41–49.

Farrell, E.F., Granja, H., Cappietti, L., Ellis, J.T., Li, B., Sherman, D.J., 2009. Wave transformation across a rock platform, Belinho, Portugal. Journal of Coastal Research SI 56, 44-48.

Kanyaya, J.I., Trenhaile, A.S., 2005. Tidal wetting and drying on shore platforms: An experimental assessment. Geomorphology 70, 129-146.

507 Kennedy, M., 2015. Where is the seaward edge? A review and definition of shore platform morphology.
508 Earth Surface Reviews 147, 99-108.
509 Kennedy, D.M., Ierodiaconou, D., Schimel, A., 2016. Granitic coastal geomorphology: applying
510 integrated terrestrial and bathymetric LiDAR with multibeam sonar to examine coastal landscape
511 evolution. Earth Surface Processes and Landforms 39, 1163-1674.
512 Lim, M, Rosser, N.J., Petley, D.N., Keen, M., 2011. Quantifying the controls and influence of tide and
513 wave impacts on coastal rock cliff erosion. Journal of Coastal Research 27, 46–56.
514 May, V.J., 1980. Hartland Quay. Coastal Geomorphology of Great Britain 28(3), 1-6.
515 Mii, H. 1962. Coastal geology of Tanabe Bay. Science Reports of the Tokoku University, Sendai,
516 Second Series, 34, 1–96.
517 Moses, C.A., 2014. The rock coast of the British Isles: shore platforms. Geological Society, London,
518 Memoirs, 40(1), 39-56.
519 Naylor, L.A., Stephenson, W.J., 2010. On the role of discontinuities in mediating shore platform erosion.
520 Geomorphology 114, 89-100.
521 Naylor, L. A., Stephenson, W. J., Trenhail, A. S., 2010. Rock coast geomorphology: Recent advances
522 and future research directions. Geomorphology 114, 3-11.
523 Norman, E. C., Rosser, N. J., Brain, M. J., Petley, D. N., Lim, M., 2013. Coastal cliff-top ground
524 motions as proxis for environmental processes. Journal of Geophysical Research 118(12), 6807-
525 6823.
526 Ogawa, H., Dickson, M.E., Kench, P.S., 2011. Wave transformation on a sub-horizontal shore platform,
527 Tatapouri, North Island, New Zealand. Continental Shelf Research 31, 1409-1419.
528 Ogawa, H., Kench, P., Dickson, M., 2012. Field measurements of wave characteristics on a near
529 horizontal shore platform, Mahia Peninsula, Norht Island, New Zealand. Geophysical Research 50,
530 179-192.
531 Ogawa, H. Kench, P., Dickson, M., 2016. Generalised observations of wave characteristics on near-
532 horizontal shore platforms: Synthesis of six case studies from the North Island, New Zealand, New
533 Zealand Geographer. doi: 10.1111/nzg.12121.
534 Orme, A.R., The raised beaches and strandlines of South Devon : field studies 1(2), 109-130.

Palamara, D. R., Dickson, M.E., Kennedy, D.M., 2007. Defining shore platform boundaries using airborne laser scan data: a preliminary investigation. Earth Surface Processes and Landforms 32, 945-953.

Porter, N.J., Trenhaile, A.S., Prestanski, K., Kanyaya, J.I., 2010a, Patterns of surface downwearing on shore platforms in eastern Canada, Earth Surf. Proc. Lands. 35, 1793-1810.

Porter, N.J., Trenhaile, A.S., Prestanski, K., Kanyaya, J.I., 2010b, Shore platform downwearing in eastern Canada: Micro-tidal Gaspé, Québec

Porter, N.J., Trenhaile, A.S., Prestanski, K., Kanyaya, J.I., 2010c, Shore platform downwearing in eastern Canada: The mega-tidal Bay of Fundy, Geomorphology 118, 1-12.

Rosser, N. J., Brain, M. J., Petley, D. N., Lim, M., Norman, E.C., 2013. Coastline retreat via progressive failure of rocky coastal cliffs. Geology 41, 939-942.

Scott, T., Masselilnk, G., Russell, P., 2011. Morphologynamic characteristics and classification of beaches in England and Wales. Marine Geology 286, 1-20.

Stephenson, W. J. and Kirk, R. M., 1998. Rates and Patterns of Erosion on Shore Platforms, Kaikoura, South Island, New Zealand. Earth Surf. Process. Landforms 23, 1071-1085.

Stephenson, W. J., 2000. Shore platforms: a neglected coastal feature? Progress in Physical Geography 24, 311-327.

Stephenson, W. J., Kirk, R. M., 2000, Development of shore platforms on Kaikouora Peninsula, South Island, New Zealand: Part Two: The role of subaerial weathering, Geomorphology 32, 43-56.Sunamura, T., 1992. Geomorphology of Rocky Coasts. John Wiley & Sons, Chichester.

Sunamura, T., 1978. A mathematical model of submarine platform development. Math. Geol. 10, 53-58.

Sunamura, T., 1992. Geomorphology of Rocky Coasts. John Wiley & Sons, Chichester.

Swantesson, J.O.H., Moses, C.A., Berg, G.E., Jansson, K.M., 2006. Methods for measuring shore platform micro-erosion: a comparison of the micro-erosion meter and laser scanner. Z. Geomorphol. 144, 1–17.

Swirad, Z.M., Rosser, N.J., Brain, M.J., Vane-Jones, E.C., 2016. What controls the geometry of rocky coasts at the local scale? Journal of Coastal Research, Special Issue 75, 612-616.

563 Trenhaile, A.S., 1972. The shore platforms of the Vale of Glamorgan, Wales. Transactions of the
564 Institute of British Geographers 56, 127–144.
565 Trenhaile, A.S., 1974. The geometry of shore platforms in England and Wales. Trans. Inst. Br. Geogr.
566 62, 129-142.
567 Trenhaile, A.S., 1980. Shore platforms: a neglected coastal feature. Progress in Physical Geography 4,
568 1-23.
569 Trenhaile, A. S., 1987. The Geomorphology of Rock Coasts. Oxford University Press, Oxford.
570 Trenhaile, A. S., 1999. The Width of Shore Platforms in Britain, Canada, and Japan. Journal of Coastal
571 Research 15, 355-364.
572 Trenhaile, A.S., 2000. Modelling the evolution of wave-cut shore platforms. Mar. Geol. 166, 163-178.
573 Trenhaile, A. S., 2005. Modeling the effect of waves, weathering and beach development on shore
574 platform development. Earth Surf. Process. Landforms 30, 613-634.
575 Trenhaile, A.S., 2008a. Modeling the role of weathering in shore platform development.
576 Geomorphology 94, 24-39.
577 Trenhaile, A.S., 2008b. The development of subhorizontal shore platforms by waves and weathering in
578 microtidal environments. Z. Geomorph. N.F. 52, 105-124.
579 Trenhaile, A.S., Layzell, M.G.J., 1981. Shore platform morphology and the tidal duration factor. Trans.
580 Inst. Br. Geogr. 6, 82-102.
581 Tsujimoto, H., 1987. Dynamic Conditions for Shore Platform Initiation. Science Reports of the Institute
582 of Geoscience University of Tsukuba A8, 45-93.
583 Young, A. P., Adams, P. N., O'Reilly, W. C., Flick, R. E., Guza, R. T., 2011. Coastal cliff ground
584 motions from local ocean swell and infragravity waves in Southern California, J. Geophys. Res.,
585 116, C09007, doi:10.1029/2011JC007175.
586 Young, A. P., Guza, R.T., O'Reilly, W.C., Burvingt, O., Flick, R.E., 2016. Observati ons of coastal cliff
587 base waves, sand levels, and cliff top shaking. Earth Surface Process and Landforms.
588 doi:10.1002/esp.3928
589 Wentworth, C.K., 1938. Marine bench-forming processes: water-level weathering. Journal of
590 Geomorphology 1, 6–32.

591